JOURNAL OF Applied Polymer SCIENCE

In Vitro Comparative Biodegradation Analysis of Salt-Leached Porous Polymer Scaffolds

Courtney E. LeBlon,[1] Riyanka Pai,[2] Caitlin R. Fodor,[3] Anne S. Golding,[3] John P. Coulter,[1] Sabrina S. Jedlicka[2,3,4]

[1]Department of Mechanical Engineering and Mechanics, Packard Laboratory, Lehigh University, Bethlehem, Pennsylvania 18015
[2]Department of Materials Science and Engineering, Whitaker Laboratory, Lehigh University, Bethlehem, Pennsylvania 18015
[3]Bioengineering Program, Lehigh University, Bethlehem, Pennsylvania 18015
[4]Center for Advanced Materials and Nanotechnology, Whitaker Laboratory, Lehigh University, Bethlehem, Pennsylvania 18015
Correspondence to: S. S. Jedlicka (E-mail: ssj207@lehigh.edu)

ABSTRACT: This study presents a comprehensive, side-by-side analysis of chemical, thermal, mechanical, and morphological changes in four polymers used in tissue engineering: poly(glycerol-sebacate) (PGS), poly(lactic acid) (PLA)/poly(ε-caprolactone) (PCL) blend, poly(lactic-*co*-glycolic acid) (PLGA), and Texin 950, a segmented polyurethane resin (PUR). Polymer foams were created using a salt-leaching technique and then analyzed over a 16-week period. Biodegradation was analyzed by examining the morphology, thermal properties, molecular weight, chemical, and mechanical properties using scanning electron microscopy, differential scanning calorimetry, gel permeation chromatography, attenuated total reflectance-Fourier transform infrared spectroscopy, thermogravimetric analysis, and compression testing. PGS underwent the most rapid degradation and was hallmarked by a decrease in compressive modulus. PLA/PCL blend and PLGA both had rapid initial decreases in compressive modulus, coupled with large decreases in molecular weight. Surface cracks were observed in the PUR samples, accompanied by a slight decrease in compressive modulus. However, as expected, the molecular weight did not decrease. These results confirm that PUR does not undergo significant degradation but may not be suitable for long-term implants. The biodegradation rates of porous PGS, PLA/PCL blend, and PLGA found in this study can guide their use in tissue engineering and other biomedical applications. © 2012 Wiley Periodicals, Inc. J. Appl. Polym. Sci. 000: 000–000, 2012

KEYWORDS: biopolymers and renewable polymers; biodegradable; biomedical applications; calorimetry; thermogravimetric analysis

Received 3 May 2012; accepted 1 July 2012; published online
DOI: 10.1002/app.38321

INTRODUCTION

A wide array of porous polymeric scaffolds have been examined for tissue engineering applications. Natural materials include collagen (cardiac and cartilage tissue engineering),[1–4] gelatin,[5,6] and alginate.[6–8] Synthetic polymers common in tissue engineering research are poly(glycolic acid) (PGA),[9–12] poly(lactic acid) (PLA),[13–15] poly(lactic-*co*-glycolic acid) (PLGA), poly(ε-caprolactone) (PCL),[16–18] poly(lactic acid-*co*-caprolactone) (PLCL),[19–21] poly(glycerol-sebacate) (PGS),[22–25] poly(hydroxy butyrate),[26,27] polyurethane resin (PUR),[28–30] and poly(propylene fumarate).[31,32] Many of the polymers that have been used in tissue engineering applications are biodegradable, including PCL, PLA, PGA, PLGA, PLCL, and PGS (among others). Often, one goal of scaffold design and development is to ensure that the rate of tissue ingrowth and the rate of polymer biodegradation are well matched for the application at hand. Although the biodegradation kinetics of the polymers listed have been examined in depth,[33–36] the scaffold fabrication between the various polymeric materials has been widely varied. In addition, the analytical methods for examining biodegradation are not always consistent between studies.

In this study, four polymers common in biomedical applications were examined (Figure 1): PGS, PLA/PCL blend, PLGA (all biodegradable at different rates), and a segmented PUR (not biodegradable). To illustrate the broad usage of these polymers in biomedical research, we have briefly reviewed each in the paragraphs below.

PGS is a bioresorbable elastomer developed by Wang et al. in 2002.[37] PGS has tunable mechanical properties, which makes it particularly interesting in tissue engineering applications. The elastic modulus and ultimate tensile strength can range from 0.056 to 1.20 MPa and 0.23 to 0.47 MPa, respectively, depending on cure temperature.[38] PGS degrades rapidly by surface

Additional Supporting Information may be found in the online version of this article.

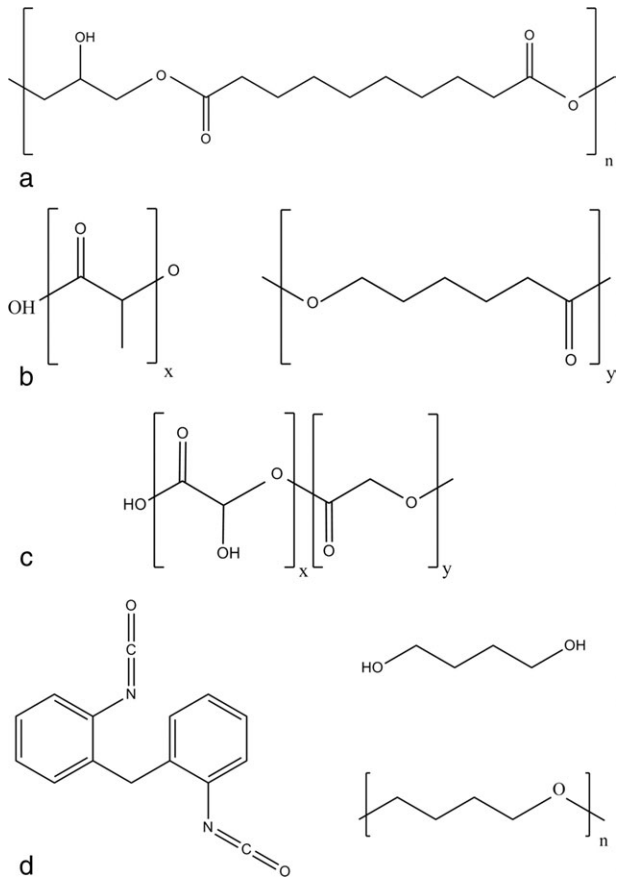

Figure 1. Chemical structures of (a) PGS, (b) PLA/PCL blend, (c) PLGA, and (d) PUR.

erosion, which results in a linear mass degradation profile,[35] regardless of degradation media composition.[37,38] PGS has a short, but very rich history as a biomaterial, *in vivo* and *in vitro*,[23,39–41] including uses in nerve guides[42] and heart valve constructs.[43] PGS has been fabricated using a number of technologies,[22–25,40,41,43–46] resulting in both porous and nonporous formats. However, while the degradation kinetics of nonporous PGS have been examined,[35,37,38,42,47] degradation kinetics of porous PGS have not yet been published.

PCL and PLA are commonly prepared as a blend or a copolymer. PCL is a semicrystalline aliphatic polyester with a relatively long degradation time (2 years), due to its hydrophobicity and crystallinity.[48] PLA is an aliphatic polyester that degrades in 2–24 months.[49,50] PLA is available in both the L and D stereoisomer forms, which affects the degradation rate, crystallinity, and molecular weight.[51] PLA/PCL blends and copolymers undergo bulk degradation by hydrolysis.[49,52–54] PLA/PCL blends have been used in a variety of ways, including drug delivery[55–58] and for nerve repair.[59,60] However, biodegradation of PLA/PCL blends in a porous format has not yet been examined.

PLGA, a copolymer of PLA and PGA, is another commonly used biodegradable polymer.[33,61–71] PGA is a crystalline aliphatic polymer that rapidly degrades (2–12 months) because of its hydrophilic nature.[50,72] PLGA has a degradation time of 1–6 months, based on the PLA/PGA ratio, as well as the crystallinity and molecular weight,[50] with a 50/50 copolymer having the most rapid degradation rate.[73] Degradation studies have also been done on PLGA porous foams *in vitro*, commonly in PBS,[33,69–71] and *in vivo*.[33] While many *in vitro* and *in vivo* studies have already been performed on PLGA, the degradation rate is highly reliant on the format (porous vs. nonporous), the ratio of PLA to PGA, and the starting molecular weight, making more research in this area crucial for understanding the potential uses of PLGA in biomedical applications.

PURs have been used in many biomedical applications,[28–30,74–76] including pacemaker lead insulation and catheters.[77] While traditionally known as nonbiodegradable, PURs are susceptible to environmental stress cracking.[78] The elastomeric properties of PUR make it a potentially useful platform in soft tissue engineering.[28–30] The polyether PUR used in this study is Texin 950, a segmented block copolymer. Segmented PURs are made up of soft segments (usually a polyol) and hard segments (a diisocyanate and chain extender) and can be tailored to have a wide range of mechanical properties. *In vivo* degradation studies have been performed on chemically similar PURs (based on methylene diphenyl diisocyanate, 1,4-butanediol, and poly(tetramethylene) ether glycol)[79,80] but to our knowledge, Texin 950 has not been the subject of inquiry. In this study, we examine the *in vitro* biodegradation of Texin 950 in a porous format, presenting data that is currently not available in the literature.

This study compares four polymers relevant to tissue engineering and presents the first biodegradation study of porous PGS, porous PLA/PCL blend, and porous PUR. While most tissue engineering scaffolds have a porous structure, many biodegradation studies do not reflect this fact. We focused our efforts on salt-leached porous scaffolds with a nominal pore size of approximately 200 μm. We performed a biodegradation analysis in simulated body fluid (SBF), under aseptic, 37°C conditions. The polymers were analyzed at specific intervals over a time course of 16 weeks, using a variety of techniques to examine chemical, thermal, mechanical, and structural changes. Our results indicate that the PGS, PLA/PCL blend, and PLGA undergo significant chemical changes indicative of biodegradation, in time periods as little as 2–4 weeks. In addition, PUR, as a nonbiodegradable polymer, exhibits cracking over time, leading to altered mechanical properties, which may impact the success of this polymer in a biomedical application. These factors are critical when considering material choice, fabrication technique, and ultimately cell integration with a biomedical device and therefore need to be studied in a systematic fashion, as described herein.

MATERIAL AND METHODS

Materials

PUR (Texin 950) was obtained from Bayer MaterialScience (Pittsburgh, PA). PLA 3051D was purchased from Natureworks (Minnetonka, MN). PCL, glycerol, sebacic acid, and dimethyl sulfoxide were acquired from Sigma Aldrich (St. Louis, MO). Glycolic acid was from TCI America (Portland, OR). Chloroform was purchased from VWR (West Chester, PA). Tetrahydrofuran (THF) and 1,1,1,3,3,3-hexamethyldisilazane were from

Acros Organics (Morris Plains, NJ). Sodium chloride (NaCl) was purchased from EMD Chemicals (Gibbstown, NJ). Zinc acetate dihydrate ($Zn(CH_3CO_2)_2{\cdot}2H_2O(I)$) was obtained from Strem Chemicals (Newburyport, MA).

Polymer/Polymer Blend Synthesis

The PGS prepolymer synthesis was adapted from established methods.[37] Briefly, equimolar (1 : 1) amounts of anhydrous glycerol and sebacic acid, which was purified via recrystallization in ethanol (3 times), were mixed in an airtight glass jar that was partially immersed in a heated silicone bath. The mixture was gradually heated to 120°C under nitrogen gas flow. The mixture was then stirred with a rotor (50 rpm) at this temperature for 24 h. The gas flow was then stopped and vacuum was applied at −20 kPa for a further 24 h.

PGA was synthesized by polycondensation, with zinc acetate dihydrate as the catalyst, as previously established.[81] This method produces a high molecular weight PGA with a number average molecular weight (M_n) of 45,000, a weight average molecular weight (M_w) of 91,000, and a crystallinity of 33%, as reported by Takahashi et al.[81]

PLGA (PLA/PGA 85 : 15) copolymer and PLA/PCL (50 : 50) blend were prepared using microwave radiation.[82] Briefly, polymers were dissolved (or suspended) in chloroform at 10% (w/v). The respective polymers were mixed prior to microwaving. This method produced a PLA/PCL blend with a PCL continuous phase and PLA microspheres ranging in diameter from 0.5 to 1 mm.

Preparation of Specimens

The porous specimens were prepared by a solvent casting/salt-leaching method.[24,67] Polymers were dissolved in solvent to yield a solution of 5% (w/v). Chloroform was used as the solvent for PLGA and PLA/PCL blend. The solvent used for PUR and PGS was THF. NaCl particles (>125μm) (90% w/v) were added to each solution. The solution was cast into rectangular molds (45 × 13 × 3 mm^3). The specimens were air dried for 48 h to allow the solvent to evaporate. The PGS specimens were then cured at 120°C for 7 days. The specimens were subsequently removed from the mold and immersed in distilled deionized water at 60°C for 72 h to leach out the salt.

DEGRADATION STUDIES

In Vitro Degradation

SBF was prepared by dissolving various reagents in ddH_2O at 37°C.[83] The SBF was filtered (0.2 μm) for sterility. Porous polymer specimens (45 × 13 × 3 mm^3) were soaked in SBF and incubated in a controlled environment (37°C, 5% CO_2). Every 2 weeks, three specimens were removed from SBF. The surface liquid was removed with a Kimwipe, and the surfaces were air dried overnight in a laminar flow hood to maintain sterility. The degradation study lasted for 16 weeks, a time period suitable for comparing polymers with variable degradation rates.

Porosity of the Initial Samples

The porosity was calculated using the densities of the porous and nonporous polymers. A total of 10 specimens were used for porosity calculations. The densities of the porous scaffolds were measured using a pycnometer. The scaffolds were dried at 70°C for 1 h prior to measurements. First, the empty, dry pycnometer was weighed (m_0). A scaffold was inserted into the pycnometer, and the weight was taken again ($m_{a,\mathrm{dry}}$). After that, the scaffold was then soaked in distilled water and placed back into the pycnometer and measured again ($m_{b,\mathrm{wet}}$). Distilled water was added so that the pycnometer was filled. The total weight was taken (m_2). The pycnometer was emptied and filled again with just distilled water (m_3). The difference between the weight of the material wet versus dry was taken ($d = m_{b,\mathrm{wet}} - m_{a,\mathrm{dry}}$) and then added to the weight of only distilled water in the pycnometer ($m_{3,\mathrm{corrected}} = m_3 + d$). The weight of the water ($m_{\mathrm{H_2O}} = m_{3,\mathrm{corrected}} - m_0$) and the weight of the scaffold ($m_S = m_{a,\mathrm{dry}} - m_0$) were calculated. Then the weight of the added water was calculated ($m'_{\mathrm{H_2O}} = m_2 - m_{a,\mathrm{dry}}$). The volume of the scaffold (V_S) was calculated using the following equation:

$$V_s = \frac{m_{\mathrm{H_2O}} - m'_{\mathrm{H_2O}}}{\rho_{\mathrm{H_2O}}}$$

The density of the scaffold, ρ_S, was then calculated using the equation below:

$$\rho_S = \frac{m_S}{V_S}$$

Finally, the porosity was calculated using the density of the nonporous polymer (ρ_P) and the density of the porous scaffold:

$$\mathrm{Porosity} = \frac{\rho_P - \rho_S}{\rho_P} \times 100.$$

Scanning Electron Microscopy. Scanning electron microscopy (SEM) was conducted using a Philips XL30 ESEM. The parameters used are as indicated at the bottom of each SEM image. Prior to imaging, the samples were sputter coated with iridium using an EMS575x Turbo Sputter Coater, using a sputter current of 20 mA for 30 s.

Mechanical Testing: Compression Tests. Compression testing is a common method for analyzing mechanical properties of porous biomedical polymers.[84–86] It has been used to evaluate biodegradation of porous PLGA.[87] Testing was performed using a Rheometrics ARES System in compression mode at a crosshead speed of 0.083 mm/s. Porous specimens were cut into 3 mm cubes for testing. The compressive modulus was calculated as the slope of the initial linear portion of the stress–strain curve. Ten compression tests were performed for each time point.

Attenuated Total Reflectance-Fourier Transform Infrared Spectroscopy. Attenuated total reflectance-Fourier transform infrared spectroscopy (ATR-FTIR) was performed on a Perkin Elmer Spectrum 100. The FTIR absorbance spectra were obtained with 16 scans per sample over the range of 4000–650 cm^{-1}, with a resolution of 4 cm^{-1}. Three samples were used for each time point.

Gel Permeation Chromatography. Gel permeation chromatography (GPC) was performed on a Waters Associates Liquid

Chromatography machine (Model #201, Milford, MA). Polymers were dissolved in THF to form 1% (w/v) solutions. The M_n and M_w data were expressed with respect to polystyrene standards. Three samples were used for each time point.

Differential Scanning Calorimetry. Differential scanning calorimetry (DSC) was used to monitor thermally induced polymer processes. It was carried out on a DuPont DSC2910 at a rate of 10°C/min; each sample was reheated. Samples weighed approximately 15 mg. The polymer samples were heated based on the areas of interest for each polymer. PGS samples were heated from −60°C to 100°C. PLA/PCL blend samples were heated from −60°C to 250°C. PLGA samples were heated from 20°C to 250°C. PUR samples were heated from −40°C to 250°C. The changes in the glass transition temperature (T_g), crystallization temperature (T_c), and melting temperature (T_m) were evaluated. One sample was used for each time point.

Thermogravimetric Analysis. Thermogravimetric analysis (TGA; TA Instruments Q500 TGA) was used to analyze thermal stability. The onset temperatures, which indicate initial temperature of mass loss, were recorded. A decrease in molecular weight is likely to be reflected in the onset temperature. The specimens were scanned from 30°C to 800°C at a heating rate of 10°C/min with a nitrogen flow rate of 40 mL/min. The weight of each sample was approximately 15 mg. Three samples were used for each time point.

RESULTS AND DISCUSSION

In Vitro Degradation

Porosity of the Specimens. The porosities of the scaffolds were calculated after determining the densities of the porous scaffolds using a pycnometer. As the scaffolds were prepared with 90% sodium chloride, a porosity of 90% would indicate that all the salt had been leached out. However, the calculated porosities of the PGS, PLA/PCL blend, PLGA, and PUR scaffolds were 80.06% (±0.02), 83.28% (±0.02), 81.24% (±0.004), and 84.16% (±0.03), respectively. This suggests that some sodium chloride was still present in the scaffolds.

SEM. SEM was used to examine the porous scaffolds during degradation (Figure 2). The images confirm that the scaffolds are highly porous, with large pores (approximately 200 μm), indicative of the salt-leaching process used to create the scaffolds. The solvent casting/salt-leaching method does not give complete interconnectivity, but this method is straightforward and simple. The surface of PGS samples no longer exhibited appreciable surface porosity by week 6. However, the cross-section showed that the porous structure was still maintained in the core of the sample. These pores disappeared by week 10. Cracks could be seen on both the surface and in the cross-section, most likely the result of the shrunken pores. By week 16, the PGS samples became gel-like. The fast degradation rate of PGS is beneficial for tissue engineering, but the loss of surface porosity early during degradation may prevent nutrient diffusion to the underlying cells. In addition, the loss of surface porosity could limit diffusion of degradation byproducts out of the scaffolds, possibly leading to toxic effects. Therefore, further testing needs to be completed with a PGS/cell hybrid to determine if cells maintained deep in the scaffolds are able to survive past the 6 week time frame.

Although the pore structure of the PLA/PCL samples was maintained on the surface and throughout the bulk for all 16 weeks, holes and increased roughness can be seen starting at week 2 of degradation. This type of structural change could be beneficial in allowing nutrient diffusion into the scaffolds (and degradation byproduct diffusion out), as well as allowing for cell–cell contact in the bulk of the scaffolds, critical to tissue engineering applications.

On the PLGA samples, cracking can be seen at week 6, and by week 10, large cracks are seen on the surface and in the bulk. Week 16 samples did not have sufficient mechanical integrity to allow for SEM preparation and imaging. Similar to the PLA/PCL blends, these changes in the structure of scaffold could improve performance with regards to cell–cell communication and diffusion. However, with both the PLA/PCL blend and the PLGA, further long-term biodegradation testing with cells would be necessary to determine how these structural changes affect cell and tissue-level integrity.

The PUR samples seemed to have an increased number of holes by week 8, and cracks can be seen by week 10. This was unexpected, given that PUR is a nonbiodegradable polymer. However, similar PUR chemistries have been shown to undergo significant surface cracking *in vivo*.[80] While the holes would possibly be beneficial for cell integration and diffusion, it is unclear if the structural changes are a result of handling or other factors. Therefore, we chose to examine chemical, thermal, and mechanical changes that result in each of the polymers chosen.

Mechanical Testing: Compression Tests. The compressive modulus of each polymer was examined during the degradation study (Figure 3). Examining the initial compressive modulus indicates that some salt may have been left behind in the scaffolds prior to placing in degradation buffer. Therefore, each polymer exhibited a dramatic drop-off in compressive strength after the first 2 weeks in culture. Initially, porous PGS had a compressive modulus of 7.24 ± 0.93 kPa. The modulus decreased by approximately 50% at week 6 (3.25 ± 0.61 kPa), which is attributed to the leaching out of any remaining salt in the scaffold. The modulus increased at week 8 to 7.61 ± 0.89 kPa, which corresponds to the substantial loss of porosity (Figure 2), then decreased again at week 10 to 5.53 ± 1.20 kPa. After 16 weeks, the PGS samples became gel-like, and therefore, the modulus could not be tested (Supporting Information for images). Wang et al.[35] reported that after 5 weeks *in vivo*, the compressive modulus of PGS implants decreased by 50%, similar to the results seen here.

Porous PLA/PCL blend had an initial compressive modulus of 136.53 ± 34.86 kPa. The modulus rapidly decreased, more than 70%, to 36.98 ± 6.28 kPa at week 2, likely due to salt leaching. It further decreased to 11.34 ± 2.55 kPa by week 16. This decrease is significant and could impact the functional ability of the scaffold during cell growth. The macroscopic structure of the scaffold did not appear significantly different, indicating that there may not have been significant pore collapse. Therefore, the degradation is attributed to bulk degradation,[50] which

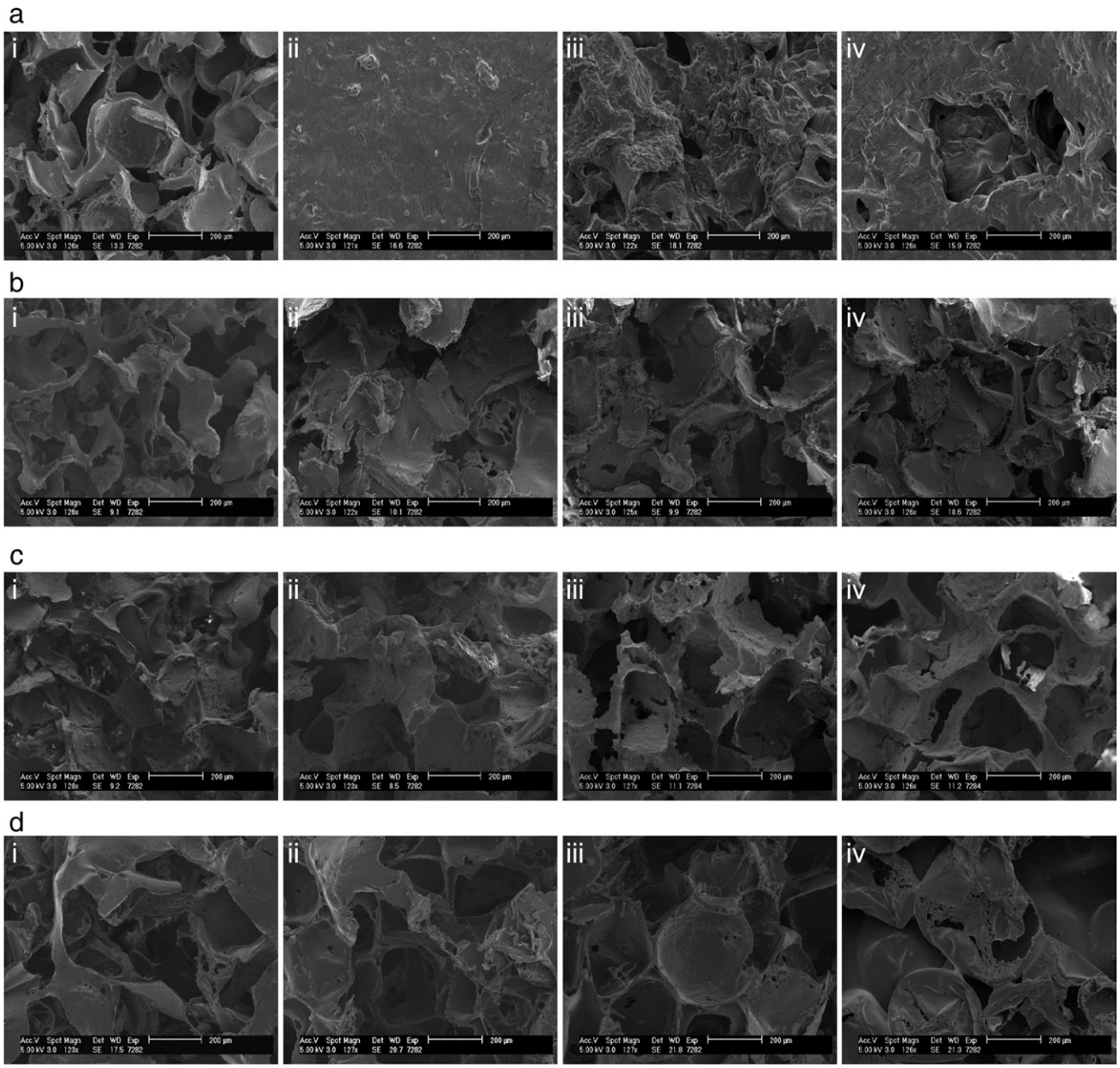

Figure 2. SEM micrographs of polymers at various time points of degradation: (a) PGS at weeks (i) 0, (ii) 6, (iii) 8, and (iv) 10, (b) PLA/PCL blend at weeks (i) 0, (ii) 2, (iii) 8, and (iv) 16, (c) PLGA at weeks (i) 0, (ii) 2, (iii) 6, and (iv) 10, and (d) PUR at weeks (i) 0, (ii) 8, (iii) 10, and (iv) 16.

is usually accompanied by a rapid loss in mechanical properties, consistent with the results seen here.

The compressive modulus of the initial porous PLGA sample was 230.39 ± 59.66 kPa. From week 0 to week 6, the modulus decreased by 85% to 34.49 ± 5.08 kPa, likely due to leftover leached salt. By week 16, the modulus had decreased to 17.37 ± 3.13 kPa, a 50% further drop from the week 6 values. Similar to PLA/PCL, PLGA is known to undergo bulk degradation; therefore, the rapid loss of mechanical integrity was expected. In addition, the PLGA macroscopic structure underwent significant changes during the degradation period, indicating a pore breakdown and ultimate collapse of the scaffold structure.

The initial compressive modulus of porous PUR was 28.08 ± 6.00 kPa. Over the course of the degradation study, the modulus decreased more than 30%, to 18.44 ± 3.81 kPa at week 16. This was a surprising finding, given that PUR does not undergo chemical degradation. However, the loss of mechanical integrity indicates that there are other factors at work in PUR incubation, which are further discussed in the data below. Regardless, the loss of mechanical integrity indicates that PUR may not be an ideal scaffold material for applications requiring a porous structure with continued mechanical integrity.

ATR-FTIR. ATR-FTIR was used to assess chemical changes occurring in the specimens during biodegradation. Each polymer was examined three times at each time point and averaged.

Applied Polymer SCIENCE

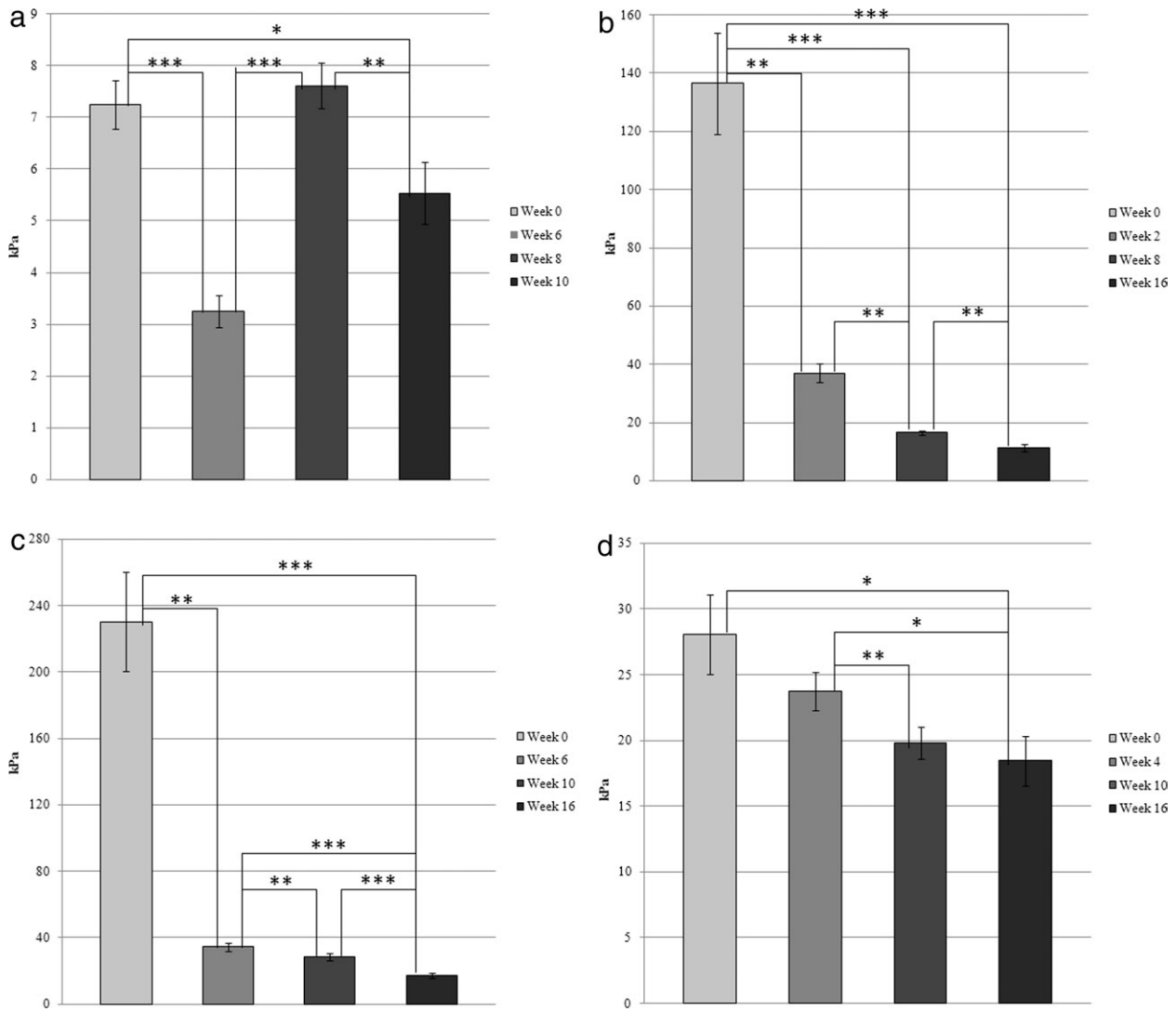

Figure 3. Compressive modulus values of (a) PGS, (b) PLA/PCL blend, (c) PLGA, and (d) PUR. PGS samples had an increase in compressive modulus from week 6 to 8, a result of the collapsed pores in the scaffold. PLA/PCL blend and PLGA had a rapid decrease in mechanical strength. PUR had a more linear decrease in compressive modulus. Error bars represent standard error (SE). $^{*}P < 0.1$, $^{**}P < 0.05$, $^{***}P < 0.01$.

Entire spectra can be seen in Supporting Information. Specific regions of interest are discussed below.

PGS has an intense stretch at approximately 1740 cm^{-1} for the double bond, C=O (Figure 4). The prepolymer displays another peak at approximately 1700 cm^{-1} for unsaturated carboxylic acids. As the crosslinks between the PGS strands break down, the peak starts to form at 1700 cm^{-1} (noticeably at week 16). This indicates breakdown of crosslinks at week 16.

PLA/PCL blend, prior to degradation, exhibits C=O stretching at 1750 cm^{-1} (due to PLA rich phase) and 1728 (due to PCL rich phase) (Figure 5). The blend also has peaks at 3000 cm^{-1} (due to PLA), 2945 cm^{-1}, and 2870 cm^{-1} (due to both PLA and PCL), representing the alkyl groups.[88] As the PLA/PCL blend degrades, the peaks due to the alkyl vibrations are maintained. A new peak forms at 3200 cm^{-1}, likely due to the

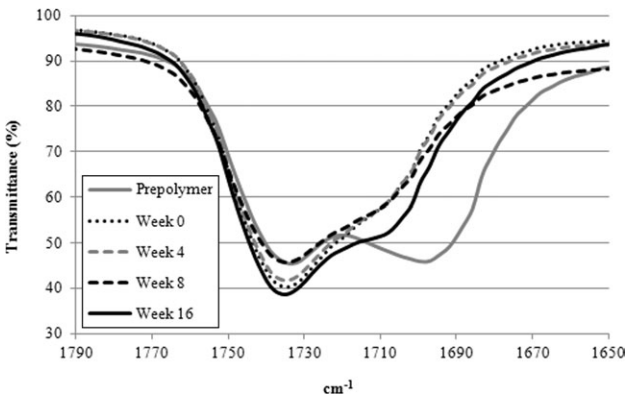

Figure 4. ATR-FTIR C=O stretch in PGS as a function of degradation time.

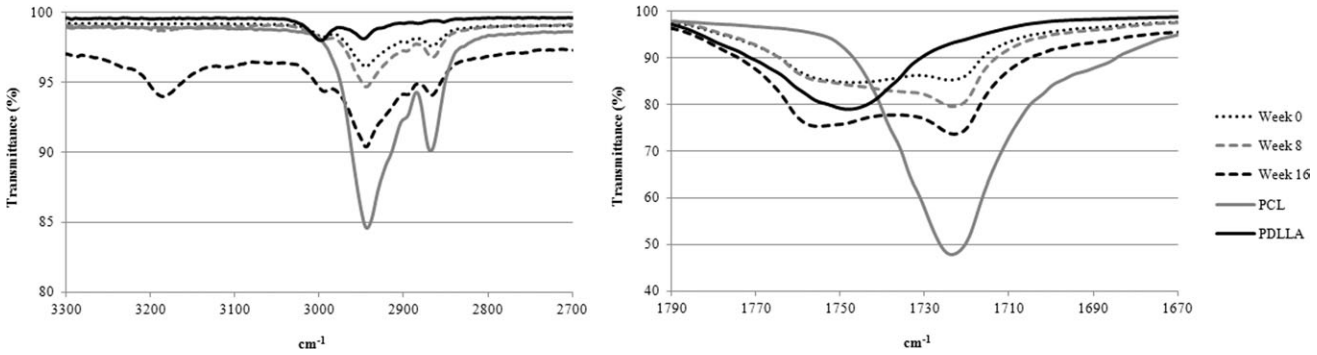

Figure 5. ATR-FTIR regions of interest for PLA/PCL blend as a function of degradation time.

increase in O—H groups as the polymer chains break. In addition, the C=O stretch exhibits an increase in the peak absorbance associated with the PLA and PCL. At week 16, the PLA/PCL blend C=O vibrational stretch indicates the evolution of increased free PLA and PCL. However, the slight shift of the peak near 1750 cm^{-1} indicates noncovalent interactions between the molecules as the polymer undergoes biodegradation.

PLGA FTIR spectra can be seen in Figure 6. During the first 6 weeks of PLGA degradation, a broad peak forms at 3400 cm^{-1}, indicating an increase in hydroxyl groups because of chain scission.[89] By week 10, the peak shifts to 3200 cm^{-1}. This indicates a decrease in hydroxyl groups, as the soluble hydroxyl end groups are leached out of the polymer. Likewise, the peak at 1750 cm^{-1}, which represents the C=O bond, increases from week 0 to 6, as chain scission occurs and carboxylic acid groups are formed. It then decreases from week 6 to 10, indicating that the carboxylic acids are being leached out, which results in significant mass loss.[89] From week 10 to 16, the C=O bond increases, most likely the result of more chain scission.

PUR has peaks at 2855 cm^{-1} and 2941 cm^{-1} for the C—H stretch (Figure 7). It also displays peaks at 1700 cm^{-1} and 1733 cm^{-1} for the C=O bond. No significant changes were seen in the C—H and C=O stretches of PUR, indicating that no major changes are occurring to the chemical bonding structure of the polymer. PUR, an MDI-based polyurethane, has semicrystalline hard segments which generally protect the urethane linkages.[79]

GPC. The molecular weights and polydispersity index (PDI) of the polymer samples were analyzed using GPC. In specimens that undergo bulk degradation (PLGA and PLA/PCL), a reduction in molecular weight is indicative of degradation in the absence of bulk weight loss. All results can be seen in Table I. For the PGS samples, only the prepolymer and week 16 were analyzed by GPC, due to the crosslinked nature of cured PGS. PGS samples through week 10 would not dissolve in THF, but the week 16 samples did dissolve, confirming that the crosslinks had entirely broken down. Additionally, the M_n and M_w decreased 14% and 12%, respectively, indicating that polymer chain length decreased compared to the prepolymer.

Because PLA/PCL is a polymer blend, two distinct peaks were expected. However, the starting molecular weights of the two polymers are similar: the M_n and M_w of PLA are 80,000 and 125,000, and the M_n and M_w of PCL are 84,000 and 119,000, respectively, as measured by GPC. Consequently, only one broad peak was found for all samples, consistent with Zhang et al.'s findings.[90] This peak became broader over the course of the biodegradation study, which is reflected in the increase in the PDI. Because only one peak was observed for the blend, the PDI does not distinguish between the two polymers and is intended to be an approximation. It is hypothesized that if the biodegradation study had been carried out longer, eventually two peaks would have become evident, as PLA is known to degrade faster than PCL. Overall, the M_n and M_w of the PLA/PCL blend decreased 45% and 29%, respectively, in the 16-week study.

The PLGA samples experienced a rapid decrease in M_n and M_w of 53% and 75%, respectively, by week 2. By week 16, the M_n and M_w had decreased 92% and 97%, respectively, from the

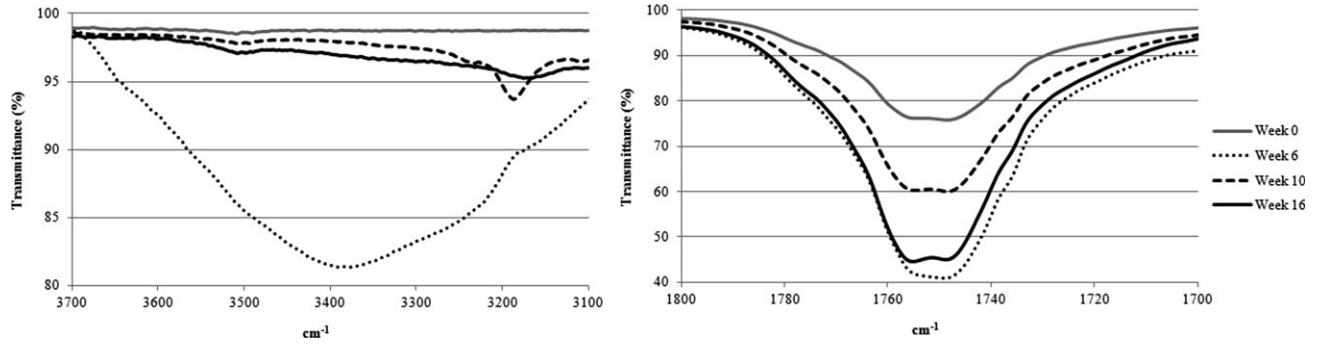

Figure 6. ATR-FTIR regions of interest for PLGA as a function of degradation time.

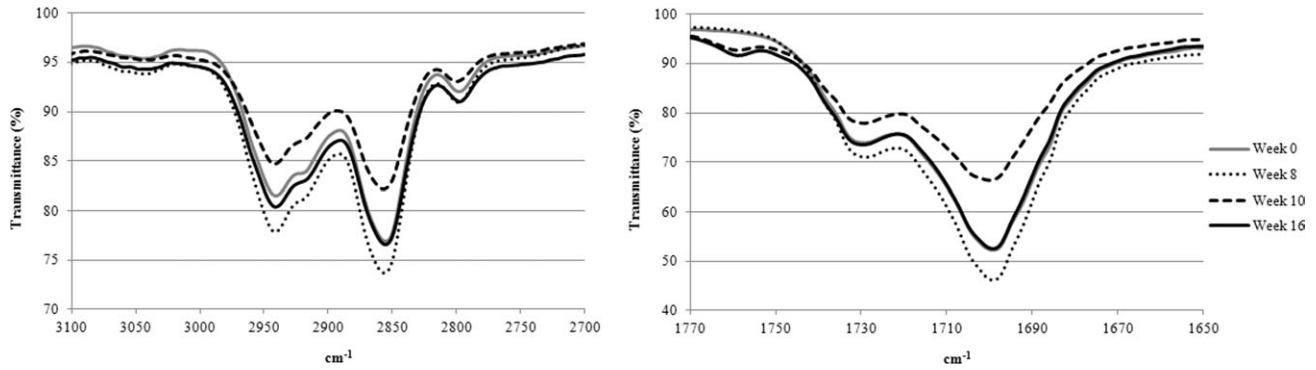

Figure 7. ATR-FTIR spectral regions for PUR as a function of degradation time.

initial samples. Interestingly, the PDI decreased throughout the experiment to a value of 1.00 by week 16, indicating that polymer chain scission had occurred very uniformly.

The PUR samples did not exhibit any decreases in M_n and M_w after 16 weeks, and the small variations seen are considered to be within the expected GPC error range of <10%. This was an expected result, given the known properties of PUR; however, it does not help to explain the loss of compressive strength that was observed.

DSC. The thermal properties of the polymer samples were analyzed using DSC. All T_g, T_m, and T_c values can be seen in Table II. All PGS samples have a T_g of approximately −30°C.[91] The prepolymer displays one melting temperature (T_m = 10°C) and one crystallization temperature (T_c = −18°C), as does the week 0 sample (T_m = 1°C, T_c = −21°C). At week 8, another melting peak is observed at 32°C. By week 16, three melting peaks are evident, at 2°C, 33°C, and 75°C. These additional peaks are attributed to the breakdown of PGS into its monomers, consistent with the ATR-FTIR and GPC data.

The T_g of PCL has been reported to be approximately −60°C,[92] while the T_g of PLA was measured as 51°C. No discernible T_g was observed in the PLA/PCL blend samples. However, the samples display two distinct melting regions, one at approximately 60°C for the PCL regions, and another at approximately 155°C, for the PLA regions, which is consistent with other reports.[93–95] An interesting finding is that the week 0 samples display one broad endotherm at 154°C for the melting of the PLA regions, while weeks 4, 8, and 16 display two endothermic peaks at approximately 150°C and 155°C, possibly indicating microphase separation. The PLA/PCL blend samples also display two distinct recrystallization temperatures, one at approximately 30°C for the PCL regions, and another at approximately 120°C for the PLA regions. The presence of two distinct melting and recrystallization regions confirm that PLA/PCL is a polymer blend.

Only one melting and crystallization region is observed in the PLGA DSC results, confirming that PLGA is a copolymer. Large decreases in the T_g, T_c, and T_m of PLGA can be seen by week 10. These observations confirm that the chain scission occurs during degradation, which results in increased chain mobility,[96] and is consistent with the GPC and ATR-FTIR results.

The T_g of the PUR samples is not easily discernable. PUR has endotherms at approximately 180°C and 200°C. Hiltz[97] reported that the endotherm at 180°C indicates the presence of microcrystalline hard segments, while the endotherm at 200°C is due to melting of crystalline hard segments resulting from increased phase separation. From week 0 to week 4, the melting and crystallization temperatures shifted to the right, suggesting that the microcrystalline hard segments may have become slightly more ordered.[97]

Table I. Change in Molecular Weight for Polymer Samples

PGS				PLA/PCL blend			
Week	M_n	M_w	PDI	Week	M_n	M_w	PDI
Prepolymer	600	2500	4.17	0	92,900	174,000	1.87
16	500	2200	4.40	4	86,300	166,500	1.93
				8	76,200	160,300	2.10
				16	51,200	123,000	2.40

PLGA				PUR			
Week	M_n	M_w	PDI	Week	M_n	M_w	PDI
0	17,900	51,200	2.86	0	77,000	235,300	3.06
2	8300	12,900	1.55	8	79,600	221,200	2.78
10	1600	1600	1.00	10	79,600	227,700	2.86
16	1400	1400	1.00	16	81,600	237,400	2.91

Table II. Changes in Thermal Properties of Polymers During Degardation

PGS					PLA/PCL blend					
	T_{m1} (°C)	T_{m2} (°C)	T_{m3} (°C)	T_c (°C)		T_{m1} (°C)	T_{m2} (°C)	T_{m3} (°C)	T_{c1} (°C)	T_{c2} (°C)
Prepolymer	10	-	-	−18	Week 0	60	-	154	31	123
Week 0	1	-	-	−21	Week 4	58	148	154	27	118
Week 8	4	32	-	−22	Week 8	60	150	156	27	119
Week 16	2	33	75	−13	Week 16	58	147	155	30	117

PLGA					PUR		
	T_g (°C)	T_c (°C)	T_m (°C)		T_{m1} (°C)	T_{m2} (°C)	T_c (°C).
Week 0	52	118	148	Week 0	178	187	117
Week 2	53	113	151	Week 4	184	203	151
Week 10	38	103	136	Week 10	188	200	150
Week 16	39	99	129	Week 16	184	199	155

TGA. Thermal stability was evaluated by TGA (Figure 8). As biodegradation occurs, thermal stability decreases, which is reflected in the onset temperature. The high weight percentage at the end of the test for the week 0 samples indicates unleached salt present in the samples and residual salt from the SBF. The onset temperatures, which indicate initial temperature of mass loss, can be seen in Table III. The onset temperature of the PGS prepolymer is 198°C. The onset temperature increases until week 8, as the weight loss curve shifts to the right. From weeks 8 to 16, the onset temperature decreases, as the curve shifts back to the left and more closely matches that of the prepolymer. All onset temperature changes are statistically

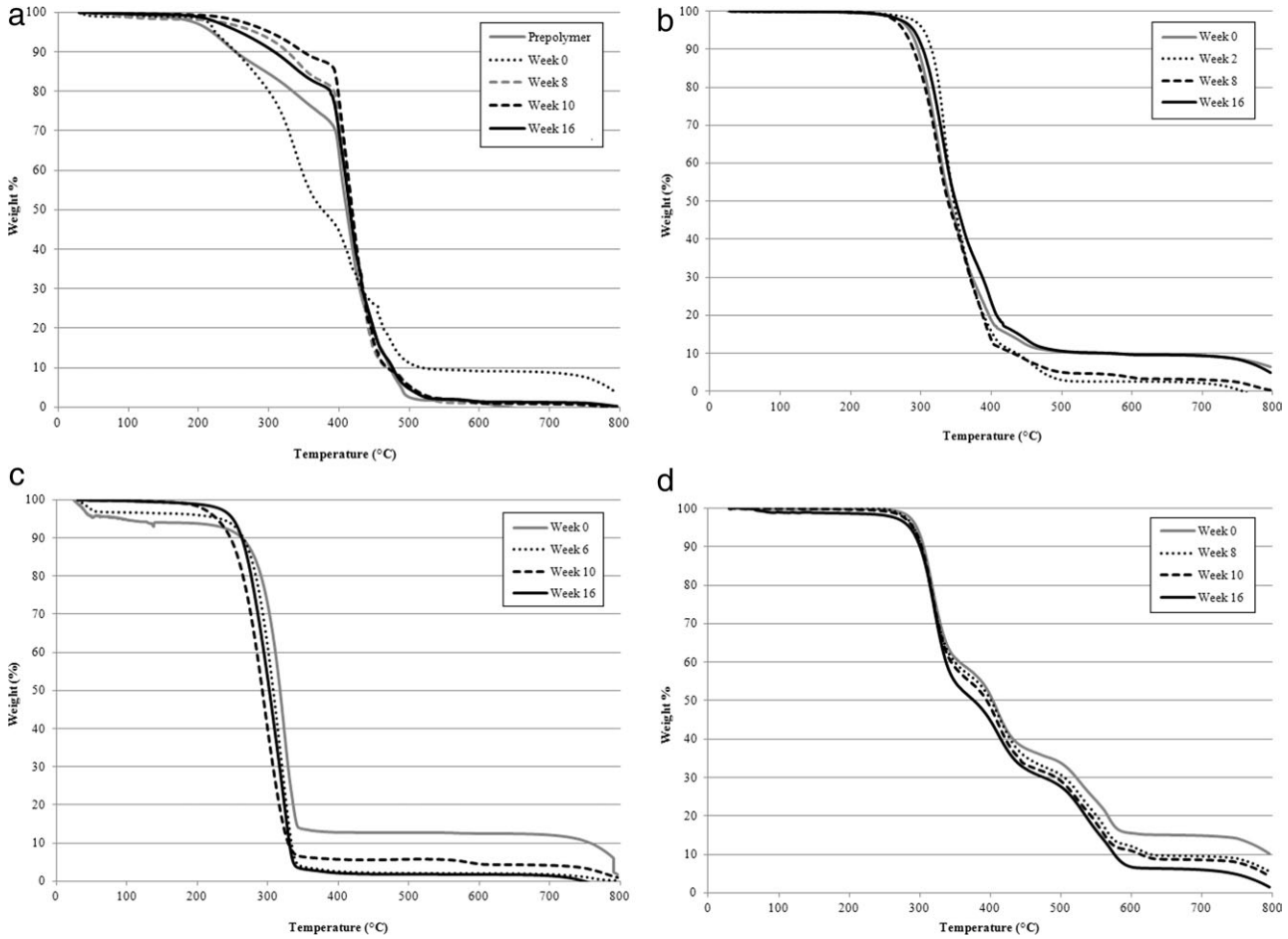

Figure 8. TGA curves of (a) PGS, (b) PLA/PCL blend, (c) PLGA, and (d) PUR.

Table III. Changes in Thermal Stability of Polymers During Degradation, as Indicated by Onset Temperature (T_O)

PGS		PLA/PCL blend		PLGA		PUR	
Week	T_o (°C)	Week	T_o (°C)	Week	T_o (°C)	Week	T_o (°C)
0	210	0	312	0	301	0	295
8	283	2	312	6	277	8	292
10	257	8	293	10	263	10	295
16	227	16	294	16	264	16	299

significant ($P < 0.01$) between the weeks analyzed. The onset temperature of PLGA decreased significantly ($P < 0.01$) over the 16-week degradation period by approximately 12%, indicating it became less thermally stable as it degraded. The onset temperature of the PLA/PCL blend samples significantly decreased ($P < 0.05$) between weeks 0 and 16 by approximately 6%. No significant decrease of onset temperature was observed for PUR over the 16-week degradation period, indicating that it maintained its thermal stability.

PGS exhibited the fastest biodegradation rate of the four polymers tested. By week 6, the surface of the samples was no longer porous, and by week 16, the polymer became gel-like. The crosslinks completely disappeared by week 16, marked by the appearance of a peak at 1700 cm^{-1}. The M_n and M_w of the prepolymer decreased from 600 and 2500, respectively, to 500 and 2200, respectively, at week 16. Additionally, two extra melting peaks were observed at week 16, which indicate monomer presence. The rapid degradation rate of PGS and the loss of porosity must be taken into account for the chosen application and structure.

The PLA/PCL blend underwent substantial degradation during the 16-week study. Increased surface roughness was observed by SEM, starting at week 2. The M_n and M_w decreased 45% and 29%, respectively, by week 16. A drastic decrease in compressive modulus of approximately 70% was observed by week 2, which can be attributed to bulk degradation and the loss of residual salt. By week 16, the compressive modulus had decreased by approximately 89%. A new peak at 3200 cm^{-1} also formed by week 16, which indicates an increase in hydroxyl groups due to chain scission.

PLGA had a major loss of mechanical integrity and molecular weight during the study. An increase in hydroxyl groups was observed during the first 6 weeks of the study, indicating chain scission. By week 16, the M_n and M_w decreased 92% and 97%. PLGA showed decreased thermal stability, as the onset temperature decreased approximately 13% by week 16. Large decreases in the T_g, T_c, and T_m of PLGA were also observed. Like the PLA/PCL blend, the PLGA samples had a drastic decrease of compressive modulus initially. By week 16, the compressive modulus decreased by approximately 92%. The severe loss of mechanical integrity may prevent its use in some applications.

PUR, a nonbiodegradable polymer, had a slight decrease in compressive modulus over the 16-week study, which may limit its use for long-term applications. An increased number of surface cracks were also observed by SEM. A shift in the T_m and T_c from weeks 0 to 4 may have signified increased order in the microcrystalline hard segments. However, no changes were observed in the chemical bonds. No decrease in thermal stability was observed.

CONCLUSIONS

This study presents a comprehensive, side-by-side analysis of chemical, thermal, mechanical, and morphological changes in four polymers used in tissue engineering. This study also presents the first report of biodegradation in porous PGS, PLA/PCL blend, and PUR. During the 16-week biodegradation study, all four polymers showed signs of degradation. PGS degraded the quickest, with complete breakdown of its crosslinks by week 16. Additionally, DSC results indicated monomer presence. As PGS has the fastest degradation rate of the polymers tested, it may be the most appropriate for many tissue engineering applications. However, the fact that the pores collapsed after 10 weeks must be taken into consideration. The PLA/PCL blend quickly experienced a rapid decrease in compressive modulus and had significant molecular weight decrease. PLGA degraded more rapidly, with significant chain scission occurring in the first 6 weeks, and showed a larger decrease in both compressive modulus and molecular weight. By week 16, the PLGA samples also lost most of their mechanical integrity and were difficult to handle. The rapid loss of mechanical properties of the PLA/PCL blend and PLGA copolymer make them unattractive candidates for tissue engineering scaffolds. Cracks and pits were seen in the SEM images of the PUR samples at week 16, which explain the 30% decrease in compressive modulus. However, its molecular weight and thermal stability did not decrease. PUR will not biodegrade in a timely manner, but it also may not be suitable for long-term implants, due to the surface flaws that result after long-term incubation. This comprehensive study presents the biodegradation properties of four polymers and can serve as a guide for their use in biomedical applications.

ACKNOWLEDGMENTS

The research was supported by NSF Lehigh Valley STEM Partnership for GK-12 Teaching Fellows: Widening the Pipeline; Grant #0638664 and NSF Grant #1014987. We also acknowledge the Lehigh University Faculty Innovation Grant (2009-2010). In addition, we would like to thank William Muschock, for his assistance with SEM imaging, Dr. Raymond Pearson for use of his equipment, and the Lehigh Emulsion Polymers Institute for GPC assistance.

REFERENCES

1. Eschenhagen, T.; Fink, C.; Remmers, U.; Scholz, H.; Wattchow, J.; Weil, J.; Zimmerman, W.; Dohmen, H. H.; Schafer, H.; Bishopric, N.; Wakatsuki, T.; Elson, E. L. *Faseb J.* **1997**, *11*, 683.
2. Frenkel, S. R.; Toolan, B.; Menche, D.; Pitman, M. I.; Pachence, J. M. *J. Bone Joint Surg-Br.* **1997**, *79B*, 831.
3. Wakitani, S.; Goto, T.; Young, R. G.; Mansour, J. M.; Goldberg, V. M.; Caplan, A. I. *Tissue Eng.* **1998**, *4*, 429.
4. Radisic, M.; Park, H.; Shing, H.; Consi, T.; Schoen, F. J.; Langer, R.; Freed, L. E.; Vunjak-Novakovic, G. *Proc. Natl. Acad. Sci. USA* **2004**, *101*, 18129.
5. Li, R. K.; Jia, Z. Q.; Weisel, R. D.; Mickle, D. A.; Choi, A.; Yau, T. M. *Circulation* **1999**, *100*, II63.
6. Awad, H. A.; Wickham, M. Q.; Leddy, H. A.; Gimble, J. M.; Guilak, F. *Biomaterials* **2004**, *25*, 3211.
7. Rowley, J. A.; Madlambayan, G.; Mooney, D. J. *Biomaterials* **1999**, *20*, 45.
8. Leor, J.; Aboulafia-Etzion, S.; Dar, A.; Shapiro, L.; Barbash, I. M.; Battler, A.; Granot, Y.; Cohen, S. *Circulation* **2000**, *102*, III56.
9. Cao, Y. L.; Vacanti, J. P.; Paige, K. T.; Upton, J.; Vacanti, C. A. *Plast. Reconstr. Surg.* **1997**, *100*, 297.
10. Freed, L. E.; Vunjaknovakovic, G.; Biron, R. J.; Eagles, D. B.; Lesnoy, D. C.; Barlow, S. K.; Langer, R. *Bio-Technology* **1994**, *12*, 689.
11. Carrier, R. L.; Papadaki, M.; Rupnick, M.; Schoen, F. J.; Bursac, N.; Langer, R.; Freed, L. E.; Vunjak-Novakovic, G. *Biotechnol. Bioeng.* **1999**, *64*, 580.
12. Vunjak-Novakovic, G.; Martin, I.; Obradovic, B.; Treppo, S.; Grodzinsky, A. J.; Langer, R.; Freed, L. E. *J. Orthop. Res.* **1999**, *17*, 130.
13. Chu, C. R.; Coutts, R. D.; Yoshioka, M.; Harwood, F. L.; Monosov, A. Z.; Amiel, D. *J. Biomed. Mater. Res.* **1995**, *29*, 1147.
14. Sittinger, M.; Reitzel, D.; Dauner, M.; Hierlemann, H.; Hammer, C.; Kastenbauer, E.; Planck, H.; Burmester, G. R.; Bujia, J. *J. Biomed. Mater. Res.* **1996**, *33*, 57.
15. Lu, H. H.; Cooper, J. A.; Manuel, S.; Freeman, J. W.; Attawia, M. A.; Ko, F. K.; Laurencin, C. T. *Biomaterials* **2005**, *26*, 4805.
16. Hutmacher, D. W.; Schantz, T.; Zein, I.; Ng, K. W.; Teoh, S. H.; Tan, K. C. *J. Biomed. Mater. Res.* **2001**, *55*, 203.
17. Ishii, O.; Shin, M.; Sueda, T.; Vacanti, J. P. *J. Thorac. Cardiovasc. Surg.* **2005**, *130*, 1358.
18. Williams, J. M.; Adewunmi, A.; Schek, R. M.; Flanagan, C. L.; Krebsbach, P. H.; Feinberg, S. E.; Hollister, S. J.; Das, S. *Biomaterials* **2005**, *26*, 4817.
19. Xu, C. Y.; Inai, R.; Kotaki, M.; Ramakrishna, S. *Biomaterials* **2004**, *25*, 877.
20. Jeong, S. I.; Kim, S. H.; Kim, Y. H.; Jung, Y.; Kwon, J. H.; Kim, B. S.; Lee, Y. M. *J. Biomater. Sci. Polym. Ed.* **2004**, *15*, 645.
21. Bhang, S. H.; Lim, J. S.; Choi, C. Y.; Kwon, Y. K.; Kim, B. *J. Biomater.Sci. Polym. Ed.* **2007**, *18*, 223.
22. Fidkowski, C.; Kaazempur-Mofrad, M. R.; Borenstein, J.; Vacanti, J. P.; Langer, R.; Wang, Y. D. *Tissue Eng.* **2005**, *11*, 302.
23. Bettinger, C. J.; Weinberg, E. J.; Kulig, K. M.; Vacanti, J. P.; Wang, Y. D.; Borenstein, J. T.; Langer, R. *Adv. Mater.* **2006**, *18*, 165.
24. Gao, J.; Crapo, P. M.; Wang, Y. D. *Tissue Eng.* **2006**, *12*, 917.
25. Engelmayr, G. C.; Cheng, M. Y.; Bettinger, C. J.; Borenstein, J. T.; Langer, R.; Freed, L. E. *Nat. Mater.* **2008**, *7*, 1003.
26. Yang, C.; Sodian, R.; Fu, P.; Luders, C.; Lemke, T.; Du, J.; Hubler, M.; Weng, Y. G.; Meyer, R.; Hetzer, R. *Ann. Thorac Surg.* **2006**, *81*, 57.
27. Asran, A. S.; Razghandi, K.; Aggarwal, N.; Michler, G. H.; Groth, T. *Biomacromolecules* **2010**, *11*, 3413.
28. Mulder, M. M.; Hitchcock, R. W.; Tresco, P. A. *J. Biomater. Sci. Polym. Ed.* **1998**, *9*, 731.
29. Schnell, A. M.; Hoerstrup, S. P.; Zund, G.; Kolb, S.; Sodian, R.; Visjager, J. F.; Grunenfelder, J.; Suter, A.; Turina, M. *J. Thorac. Cardiovasc. Surg.* **2001**, *49*, 221.
30. Grad, S.; Kupcsik, L.; Gorna, K.; Gogolewski, S.; Alini, M. *Biomaterials* **2003**, *24*, 5163.
31. Fisher, J. P.; Vehof, J. W. M.; Dean, D.; van der Waerden, J. P. C. M.; Holland, T. A.; Mikos, A. G.; Jansen, J. A. *J. Biomed. Mater. Res.* **2002**, *59*, 547.
32. Vehof, J. W. M.; Fisher, J. P.; Dean, D.; van der Waerden, J. P. C. M.; Spauwen, P. H. M.; Mikos, A. G.; Jansen, J. A. *J. Biomed. Mater. Res.* **2002**, *60*, 241.
33. Lu, L.; Peter, S. J.; Lyman, M. D.; Lai, H. L.; Leite, S. M.; Tamada, J. A.; Uyama, S.; Vacanti, J. P.; Langer, R.; Mikos, A. G. *Biomaterials* **2000**, *21*, 1837.
34. Kenley, R. A.; Lee, M. O.; Mahoney, T. R.; Sanders, L. M. *Macromolecules* **1987**, *20*, 2398.
35. Wang, Y. D.; Kim, Y. M.; Langer, R. *J. Biomed. Mater. Res. Part A* **2003**, *66A*, 192.
36. Jeong, S. I.; Kim, B. S.; Kang, S. W.; Kwon, J. H.; Lee, Y. M.; Kim, S. H.; Kim, Y. H. *Biomaterials* **2004**, *25*, 5939.
37. Wang, Y.; Ameer, G. A.; Sheppard, B. J.; Langer, R. *Nat. Biotechnol.* **2002**, *20*, 602.
38. Chen, Q. Z.; Bismarck, A.; Hansen, U.; Junaid, S.; Tran, M. Q.; Harding, S. E.; Ali, N. N.; Boccaccini, A. R. *Biomaterials* **2008**, *29*, 47.
39. Sun, Z.; Chen, C.; Sun, M.; Ai, C.; Lu, X.; Zheng, Y.; Yang, B.; Dong, D. *Biomaterials* **2009**, *30*, 5209.
40. Motlagh, D.; Yang, J.; Lui, K. Y.; Webb, A. R.; Ameer, G. A. *Biomaterials* **2006**, *27*, 4315.
41. Kemppainen, J. M.; Hollister, S. J. *J. Biomed. Mater. Res. Part A* **2010**, *94A*, 9.
42. Sundback, C. A.; Shyu, J. Y.; Wang, Y. D.; Faquin, W. C.; Langer, R. S.; Vacanti, J. P.; Hadlock, T. A. *Biomaterials* **2005**, *26*, 5454.
43. Sales, V. L.; Engelmayr, G. C., Jr.; Johnson, J. A., Jr.; Gao, J.; Wang, Y.; Sacks, M. S.; Mayer, J. E. *Circulation* **2007**, *116*, I55.
44. Yi, F.; LaVan, D. A. *Macromol. Biosci.* **2008**, *8*, 803.

45. Radisic, M.; Park, H.; Chen, F.; Salazar-Lazzaro, J. E.; Wang, Y.; Dennis, R.; Langer, R.; Freed, L. E.; Vunjak-Novakovic, G. *Tissue Eng.* **2006**, *12*, 2077.
46. Bettinger, C. J.; Orrick, B.; Misra, A.; Langer, R.; Borenstein, J. T. *Biomaterials* **2006**, *27*, 2558.
47. Pomerantseva, I.; Krebs, N.; Hart, A.; Neville, C. M.; Huang, A. Y.; Sundback, C. A. *J. Biomed. Mater. Res. Part A* **2009**, *91A*, 1038.
48. Middleton, J. C.; Tipton, A. J. *Biomaterials* **2000**, *21*, 2335.
49. Pitt, C. G.; Gratzl, M. M.; Kimmel, G. L.; Surles, J.; Schindler, A. *Biomaterials* **1981**, *2*, 215.
50. Gunatillake, P. A.; Adhikari, R. *Eur. Cell Mater.* **2003**, *5*, 1.
51. Garlotta, D. *J. Polym. Environ.* **2001**, *9*, 63.
52. Gan, Z. H.; Yu, D. H.; Zhong, Z. Y.; Liang, Q. Z.; Jing, X. B. *Polymer* **1999**, *40*, 2859.
53. Liu, L. J.; Li, S. M.; Garreau, H.; Vert, M. *Biomacromolecules* **2000**, *1*, 350.
54. Wang, L.; Ma, W.; Gross, R.; McCarthy, S. *Polym. Degrad. Stabil.* **1998**, *59*, 161.
55. Chandy, T.; Wilson, R.; Rao, G.; Das, G. *J. Biomater. Appl.* **2002**, *16*, 275.
56. Cai, Q.; Bei, J.; Wang, S. *Polym. Adv. Technol.* **2002**, *13*, 534.
57. Fialho, S. L.; Prado, L. M. F.; Ferreira, D. S.; Pereira, B. G.; Faraco, A. A. G.; Silva-Cunha, A. *Lat. Am. J. Pharm.* **2010**, *29*, 694.
58. Shen, Y.; Sun, W.; Zhu, K.; Shen, Z. *J. Biomed. Mater. Res.* **2000**, *50*, 528.
59. Sun, M.; Downes, S. *J. Mater. Sci. Mater. Med.* **2009**, *20*, 1181.
60. Sun, M.; Kingham, P. J.; Reid, A. J.; Armstrong, S. J.; Terenghi, G.; Downes, S. *J. Biomed. Mater. Res. Part A* **2010**, *93A*, 1470.
61. Ishaug, S. L.; Crane, G. M.; Miller, M. J.; Yasko, A. W.; Yaszemski, M. J.; Mikos, A. G. *J. Biomed. Mater. Res.* **1997**, *36*, 17.
62. Stitzel, J.; Liu, L.; Lee, S. J.; Komura, M.; Berry, J.; Soker, S.; Lim, G.; Van Dyke, M.; Czerw, R.; Yoo, J. J.; Atala, A. *Biomaterials* **2006**, *27*, 1088.
63. Lu, L.; Garcia, C.; Mikos, A. *J. Biomed. Mater. Res.* **1999**, *46*, 236.
64. Ishaug-Riley, S. L.; Okun, L. E.; Prado, G.; Applegate, M. A.; Ratcliffe, A. *Biomaterials* **1999**, *20*, 2245.
65. Fu, K.; Pack, D. W.; Klibanov, A. M.; Langer, R. *Pharm. Res.* **2000**, *17*, 100.
66. Cohen, S.; Yoshioka, T.; Lucarelli, M.; Hwang, L.; Langer, R. *Pharm. Res.* **1991**, *8*, 713.
67. Mikos, A. G.; Thorsen, A. J.; Czerwonka, L. A.; Bao, Y.; Langer, R.; Winslow, D. N.; Vacanti, J. P. *Polymer* **1994**, *35*, 1068.
68. Park, T. G. *Biomaterials* **1995**, *16*, 1123.
69. Thomson, R. C.; Yaszemski, M. J.; Powers, J. M.; Mikos, A. G. *J. Biomater. Sci. Polym. Ed.* **1995**, *7*, 23.
70. Widmer, M.; Gupta, P.; Lu, L.; Meszlenyi, R.; Evans, G.; Brandt, K.; Savel, T.; Gurlek, A.; Patrick, C.; Mikos, A. *Biomaterials* **1998**, *19*, 1945.
71. Wu, X. S.; Wang, N. *J. Biomater. Sci. Polym. Ed.* **2001**, *12*, 21.
72. Webb, A. R.; Yang, J.; Ameer, G. A. *Expert Opin. Biol. Ther.* **2004**, *4*, 801.
73. Miller, R. A.; Brady, J. M.; Cutright, D. E. *J. Biomed. Mater. Res.* **1977**, *11*, 711.
74. Gorna, K.; Gogolewski, S. *J. Biomed. Mater. Res. Part A* **2006**, *79A*, 128.
75. McDevitt, T. C.; Woodhouse, K. A.; Hauschka, S. D.; Murry, C. E.; Stayton, P. S. *J. Biomed. Mater. Res. Part A* **2003**, *66A*, 586.
76. Alperin, C.; Zandstra, P. W.; Woodhouse, K. A. *Biomaterials* **2005**, *26*, 7377.
77. Zdrahala, R. J.; Zdrahala, I. J. *J. Biomater. Appl.* **1999**, *14*, 67.
78. Stokes, K.; McVenes, R.; Anderson, J. M. *J. Biomater. Appl.* **1995**, *9*, 321.
79. Hergenrother, R.; Wabers, H.; Cooper, S. *Biomaterials* **1993**, *14*, 449.
80. Brandwood, A.; Meijs, G.; Gunatillake, P.; Noble, K.; Schindhelm, K.; Rizzardo, E. *J. Biomater. Sci. Polym. Ed.* **1994**, *6*, 41.
81. Takahashi, K.; Taniguchi, I.; Miyamoto, M.; Kimura, Y. *Polymer* **2000**, *41*, 8725.
82. Pandey, A.; Pandey, G. C.; Aswath, P. B. *J. Mech. Behav. Biomed. Mater.* **2008**, *1*, 227.
83. Kokubo, T.; Kushitani, H.; Sakka, S.; Kitsugi, T.; Yamamuro, T. *J. Biomed. Mater. Res.* **1990**, *24*, 721.
84. Lam, C.; Mo, X.; Teoh, S.; Hutmacher, D. *Mater. Sci. Eng. C Biomimetic Supramol. Syst.* **2002**, *20*, 49.
85. Mathieu, L.; Mueller, T.; Bourban, P.; Pioletti, D.; Muller, R.; Manson, J. *Biomaterials* **2006**, *27*, 905.
86. Kang, Y.; Yang, J.; Khan, S.; Anissian, L.; Ameer, G. *J. Biomed. Mater. Res. Part A* **2006**, *77A*, 331.
87. Wu, L. B.; Ding, J. D. *Biomaterials* **2004**, *25*, 5821.
88. Garkhal, K.; Verma, S.; Jonnalagadda, S.; Kumar, N. *J. Polym. Sci. Part A Polym. Chem.* **2007**, *45*, 2755.
89. Tan, H. Y.; Widjaja, E.; Boey, F.; Loo, S. C. J. *J. Biomed. Mater. Res. Part B Appl. Biomater.* **2009**, *91B*, 433.
90. Zhang, L.; Xiong, C.; Deng, X. *J. Appl. Polym. Sci.* **1995**, *56*, 103.
91. Jaafar, I. H.; Ammar, M. M.; Jedlicka, S. S.; Pearson, R. A.; Coulter, J. P. *J. Mater. Sci.* **2010**, *45*, 2525.
92. Ye, W. P.; Du, F. S.; Jin, J. Y.; Yang, J. Y.; Xu, Y. *React. Funct. Polym.* **1997**, *32*, 161.
93. Chen, C.; Chueh, J.; Tseng, H.; Huang, H.; Lee, S. *Biomaterials* **2003**, *24*, 1167.
94. Lopez-Rodriguez, N.; Lopez-Arraiza, A.; Meaurio, E.; Sarasua, J. R. *Polym. Eng. Sci.* **2006**, *46*, 1299.
95. Park, J.; Todo, M. *J. Mater. Sci.* **2011**, *46*, 7850.
96. Mehta, R.; Thanoo, B.; DeLuca, P. *J. Control. Release* **1996**, *41*, 249.
97. Hiltz, J. A. Defence Research Establishment Atlantic TM98/222, Grant 1GH, 1–38, **1998**.